sustainability

MDPI

Article

Scenario-Based Modeling of Hydrodynamics and Water Exchange Under Ecological Water Replenishment in Topographically Heterogeneous Baiyangdian Lake

Yuanyan Ma [1,2], Liting Zhang [1,*], Yongtao Zhu [2], Xinwang Li [2], Yingdong Guo [1] and Yunning Chi [3]

[1] Key Laboratory of Roads and Railway Engineering Safety Control, Ministry of Education, Shijiazhuang Tiedao University, Shijiazhuang 050043, China
[2] Hebei Institute of Water Science, Shijiazhuang 050043, China
[3] First Institute of Oceanography, Qingdao 266061, China
* Correspondence: zhanglt0709@sina.com

Abstract

Water circulation and exchange in shallow lakes can be restricted by complex bathymetry and human activities. However, the interaction between dynamic water replenishment strategies and complex bathymetry remains unclear. This study developed a two-dimensional hydrodynamic model of the highly fragmented Baiyangdian Lake. Using the spring water replenishment process in 2024 as the baseline, it simulated the effects of six control scenarios covering total replenishment volume, duration and the temporal distribution of inflow on the flow field and water exchange percentage. The results showed the following: (1) Increasing replenishment volume to 1.5 times the baseline raised the main-lake active water area fraction (flow velocity > 0.60 cm s^{-1}) from 31.37% to 40.71%. The main-lake water exchange percentage reached 49.34% on day 32. (2) The water exchange percentage exhibited strong spatial heterogeneity, and the relative performance of the tested scenarios depended on local topographic resistance. Short-duration or concentrated replenishment may promote water exchange in topographically constrained areas, whereas open-channel areas may benefit from longer-duration replenishment. (3) This study characterized the simulated responses of shallow lakes to water replenishment regulation under complex microtopography, providing hydrodynamic evidence for sustainable, spatially differentiated replenishment planning in fragmented wetlands.

Keywords: ecological water replenishment regulation; hydrodynamic modeling; water exchange percentage; topographic heterogeneity; pulse effect; Baiyangdian lake

Check for updates

Academic Editor: Giovanni De Feo

Received: 8 October 2026
Revised: 5 November 2026
Accepted: 6 November 2026
Published: 13 November 2026

Copyright: © 2026 by the authors. Licensee MDPI, Basel, Switzerland. This article is an open access article distributed under the terms and conditions of the Creative Commons Attribution (CC BY) license.

1. Introduction

Shallow lakes and wetland ecosystems play an irreplaceable role in water conservation, climate regulation, and maintaining regional biodiversity [1,2]. However, under the combined impacts of global climate change and intensive human activities, many large shallow lakes around the world are facing serious challenges, including sharp declines in inflow, reduced water connectivity, and degradation of the aquatic environment [3,4]. In addition, lake geometry has been recognized as an important factor controlling hydrodynamic characteristics and nutrient distribution [5], particularly in shallow lakes with complex morphologies. Ecological water replenishment, as a direct and effective engineering measure for restoring degraded lake ecosystems, has been widely applied in global water resource management practices [6,7]. During ecological water replenishment, improved hydrodynamic characteristics and higher water exchange efficiency are the main drivers of nutrient

transport, diffusion, and degradation, which in turn improve water quality and promote ecological restoration [8,9]. Therefore, quantifying how ecological water replenishment affects lake hydrodynamics and water exchange is important for optimizing water allocation and supporting sustainable lake water management.

As the largest natural shallow lake wetland on the North China Plain, Baiyangdian plays an important role in maintaining regional ecological balance. Since the 1980s, excessive water resource development in the watershed and water interception by upstream reservoirs have caused a sharp decline in inflow to Baiyangdian Lake, resulting in severe impairment of ecosystem functions [10]. More importantly, long-term agricultural reclamation and aquaculture activities have led to the widespread distribution of embankments, dikes, and reed beds in Baiyangdian, creating a highly complex and fragmented landscape that severely restricts natural water flow and exchange [11]. Following the establishment of the Xiong'an New Area in 2017, Baiyangdian, as a core area for ecological development, gained a historic opportunity for restoration. Through cross-basin water diversion projects, including the "Yellow River Diversion to Hebei for Baiyangdian Replenishment" project and ecological water replenishment from the Middle Route of the South-to-North Water Diversion Project, Baiyangdian has gradually developed a regular water replenishment system with multiple water sources and pathways [1,12]. By 2024, after several inflowing rivers were fully connected, the water surface area of Baiyangdian Lake had recovered to more than 250 km^2, and its water level had been effectively maintained.

With the implementation of large-scale ecological water replenishment projects, researchers worldwide have investigated their ecological and environmental effects. Previous studies have mainly focused on the large-scale ecological effects of ecological water replenishment, including lake water level recovery, water quality improvement, and aquatic vegetation succession [7,13]. Numerical models have been widely used to study hydrodynamic processes and solute transport in large shallow lakes [14]. In terms of hydrodynamics, previous studies have used numerical models to demonstrate that inter-basin water transfers can significantly enhance overall water circulation in lakes [8,15]. However, water resources available for ecological water replenishment are limited. Previous studies have optimized replenishment channels, periods, and water allocation [4], and examined long-term changes in lake water exchange [16]. These studies provide a basis for further assessing how event-scale replenishment schedules affect the correspondence between active water area and tracer-based exchange. In highly fragmented lakes, this assessment also needs to account for contrasting topographic constraints among subregions [11].

The joint effects of replenishment timing and topographic constraints on water exchange in fragmented shallow lakes remain insufficiently understood. Here, we developed a two-dimensional MIKE 21 FM model of Baiyangdian using high-resolution measured topography [16,17]. Six scenarios based on the spring 2024 replenishment event varied total volume, duration, and temporal distribution of inflow. We evaluated active water zone area and tracer-based exchange metrics across the main lake and subregions [18,19]. This study addresses two research questions: (1) How do replenishment volume, duration, and temporal distribution of inflow affect active water area and tracer-based water exchange? (2) Does greater hydrodynamic activation consistently correspond to greater water exchange across subregions with contrasting topographic constraints?

2. Overview of the Study Area and Data Sources

2.1. Overview of the Study Area

Baiyangdian is located in the Qing River Basin of the Hai River Basin. It is 39.5 km long from east to west and 28.5 km wide from north to south, and it covers approximately 366 km^2. Baiyangdian contains 143 water bodies of varying sizes and approximately 3700 channels,

forming a highly fragmented network [20]. The taxonomic and functional diversity of benthic communities shows clear spatial gradients [21], reflecting highly heterogeneous habitat structure in this area. The terrain of Baiyangdian is higher in the west and lower in the east, and higher in the south and lower in the north. The topography of Baiyangdian is gentle and the average elevation is approximately 7.7 m. The region has a temperate, semi-arid continental monsoon climate. Extreme temperatures range from −26.7 °C to 40.7 °C. The mean annual temperature is 12.2 °C, and the annual average precipitation is 529.7 mm [1].

Since the establishment of Xiong'an New Area in 2017, Baiyangdian has developed an ecological water replenishment system based on coordinated scheduling of multiple water sources, including Yellow River water diversion and the Middle Route of the South-to-North Water Diversion Project, helping alleviate water shortages [4,12]. Currently, the main rivers that regularly discharge into Baiyangdian Lake include the Baigou Diversion Channel, Tang River, Fu River, Cao River, and Bao River, while the Zhao Wang New River serves as the main flood discharge outlet. Considering the highly complex topography of Baiyangdian and the presence of seasonal dry areas along its margins, this study focused the simulation and analysis on the main-lake area, where water connectivity is relatively high and ecological functions are important. The study area includes six representative subregions: Shaochedian, Nanliuzhuang, Gudingdian, Duancun, Quantou, and Caiputai. These subregions were selected to compare replenishment responses across areas with different topographic constraints and hydraulic connectivity. The geographical location and zoning information of the study area are shown in Figure 1. Previous studies have investigated the spatiotemporal variations in water quality and their driving mechanisms in Baiyangdian [22], providing a basis for evaluating the hydrodynamic effects of water replenishment.

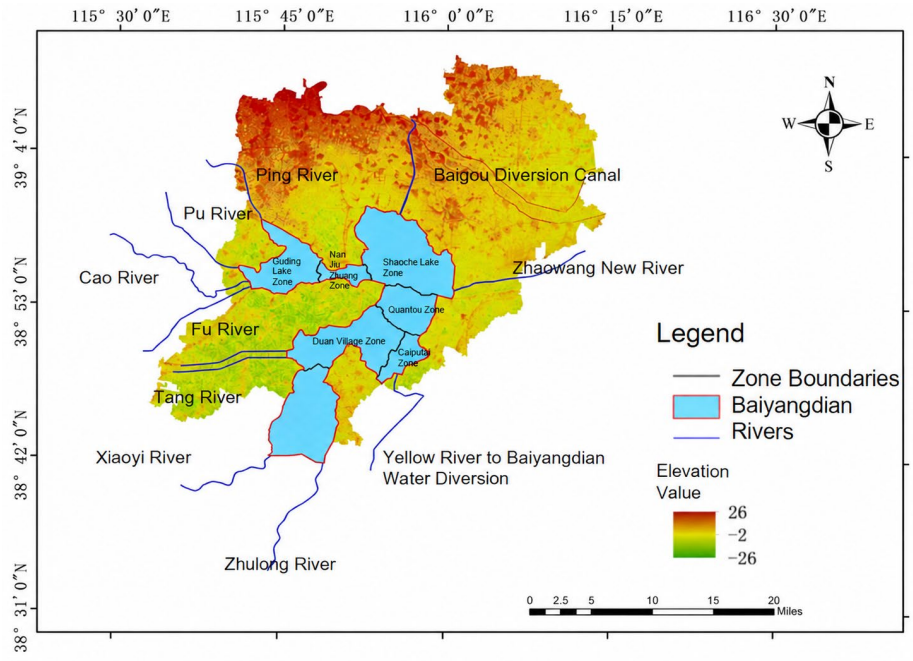


Figure 1. Overview of the study area.

2.2. Data Sources

The multi-source datasets used for developing the two-dimensional hydrodynamic model and conducting scenario simulations in this study mainly include:

(1) Hydrological data: Boundary discharge and observed water level data required for model calibration and validation, provided by the Xiong'an New Area Hydrological Survey and Research Center.
(2) Meteorological boundary data: Driving variables including precipitation, wind speed, and wind direction, obtained from the National Meteorological Observation Station in Anxin County, Baoding City. These observations were used to prepare the wind and rainfall input files, which represented the temporal variation in meteorological forcing.
(3) Topographic data: High-resolution measured digital elevation model (DEM) data required for model mesh generation, provided by the Hebei Provincial Water Resources Science Research Institute.
(4) Hydrogeological parameters: Loss parameters including water surface evaporation and sediment seepage in the study area, derived from historical observation records of the Baiyangdian Basin compiled by the Hebei Provincial Water Resources Science Research Institute.

3. Research Methods

3.1. Characteristics of Water Exchange and Calculation Methods

Water exchange characteristics are crucial for quantitative evaluation of hydrodynamic connectivity and self-purification capacity. We applied an advection–dispersion model with conservative tracers—solutes that do not settle or react biogeochemically—to quantify water exchange [23,24]. The governing equation is:

$$\frac{\partial C}{\partial t} + u\frac{\partial C}{\partial x} + v\frac{\partial C}{\partial y} = \frac{\partial}{\partial x}\left(D_x\frac{\partial C}{\partial x}\right) + \frac{\partial}{\partial y}\left(D_y\frac{\partial C}{\partial y}\right)$$

In the equation, C is the conservative tracer concentration, u and v are velocity components, and Dx and Dy are dispersion coefficients.

In this framework, water exchange depends mainly on advection from external freshwater input and turbulent dispersion caused by flow shear [18]. Water renewal time (WRT) is a key parameter for this process. We followed the widely used e-folding time criterion in physical oceanography and aquatic environmental studies [18,19]. Under this criterion, effective exchange is assumed to occur when the concentration of a conservative tracer, initially released uniformly in a given area, decays exponentially to 1/e of its initial value—that is, $C(t)/C_0 \approx 0.37$ (or 37%). The time required to reach this threshold and the proportion of the assessed water area meeting it were used as the core quantitative indicators of replenishment performance.

Water exchange was simulated through advection and dispersion of a conservative tracer [18]. The tracer was initially distributed uniformly within the assessed water region and was assumed not to settle or undergo biogeochemical reactions. The uniform initial tracer concentration was $C_0 = 1$ mg L^{-1}. The normalized tracer concentration was defined as

$$c(x, y, t) = \frac{C(x, y, t)}{C_0}$$

where C(x, y, t) is the tracer concentration at location (x, y) and time t, and C_0 is its uniform initial concentration. The normalized concentration c is dimensionless and initially equals 1 within the initialized region.

Water renewal time was defined using the e-folding criterion [18,19], as the elapsed time required for tracer concentration to decrease to 1/e of C_0. The corresponding concentration threshold is

$$c \leq \frac{1}{e} \approx 0.37$$

With $C_0 = 1$ mg L^{-1}, this criterion corresponds to an absolute tracer concentration threshold of:

$$C_{threshold} = \frac{C_0}{e} \approx 0.3679 \approx 0.37$$

At each reporting time, the water exchange percentage was defined as the proportion of the assessed water area meeting this criterion:

$$R_A(t) = \frac{A_{ex}(t)}{A_{assess}} \times 100\%$$

Here, $A_{ex}(t)$ is the water area satisfying $C/C_0 \leq 1/e$ at time t, and A_{assess} is the total water area used for the corresponding assessment. This calculation was applied to the main-lake area and each subregion. The reported percentages therefore describe the spatial extent of water renewal according to the e-folding concentration threshold. Constant, spatially uniform horizontal tracer dispersion coefficients were prescribed as 1 m^2 s^{-1}. The tracer concentration at the inflow boundaries was fixed at 0 mg L^{-1}. An advective outflow condition was applied to tracer transport, allowing tracer to leave the computational domain without prescribing an outlet concentration.

3.2. Development and Validation of a Hydrodynamic Model

3.2.1. Governing Equations and Mesh Discretization

A hydrodynamic model of Baiyangdian was developed using the MIKE 21 Flow Model FM within MIKE Zero 2014 (version 14.0.7349, 64-bit) [25]. The model solves the two-dimensional shallow water equations (SWEs). These equations are derived by depth-integrating the three-dimensional incompressible Reynolds-averaged Navier–Stokes equations under the Boussinesq and hydrostatic pressure assumptions. They comprise the continuity and momentum conservation equations [26].

An unstructured mesh was used to represent the fragmented morphology of Baiyangdian. The mesh was generated automatically in MIKE using measured digital elevation model (DEM) data. It contained approximately 410,000 mesh elements and 820,000 mesh nodes. Local mesh refinement was applied in complex waterways and flow-constriction zones. Individual element areas ranged from 10 m^2 to 4000 m^2. Mesh independence was not assessed; therefore, the sensitivity of simulated flow velocities and area-based water exchange percentages to mesh resolution remains unquantified.

The numerical settings used in the hydrodynamic model are summarized in Table 1. The drying, flooding, and wetting depth thresholds were set to 0.005, 0.05, and 0.10 m, respectively. The overall model time interval was set to 30 s. Time integration used a second-order explicit Runge–Kutta scheme. Both the hydrodynamic and tracer advection–dispersion calculations employed adaptive internal time stepping, with a critical Courant–Friedrichs–Lewy (CFL) number of 0.80 and minimum and maximum permitted time steps of 0.01 and 30 s, respectively.

Table 1. Initial and final model settings.

Parameter or Setting	Unit	Initial	Final	Classification
Manning number (M = 1/n)	$m^{1/3}$ s^{-1}	25	32	Adjusted parameter
Smagorinsky coefficient	–	0.28	0.25	Adjusted parameter
Drying depth	m	0.005	0.005	Fixed setting
Flooding depth	m	0.05	0.05	Fixed setting
Wetting depth	m	0.1	0.1	Fixed setting
Constant wind-drag coefficient	–	0.0016	0.0013	Adjusted parameter
Initial water level	m	6.55	6.58	Initial condition
Sediment seepage rate	mm d^{-1}	1.5	1.2	Water-balance input
Maximum CFL number	–	0.8	0.8	Fixed setting

Based on the topography of the study area, inflow boundaries were assigned to higher-elevation locations, while outflow boundaries were assigned to lower-elevation locations. Inflow discharges were defined according to the spring 2024 ecological water replenishment baseline and the volume, duration, and temporal distribution specified for each scenario in Table 2. A constant discharge boundary condition was prescribed at the outlet, with $Q = -0.5\ m^3\ s^{-1}$. The initial water level was set to 6.58 m. Bed resistance, wind drag, and sediment seepage were assigned the final parameter values reported in Table 1. All remaining numerical options retained the default settings of MIKE 21 FM.

Table 2. Six scenarios.

Scenario	ID	Total Replenishment Volume	Replenishment Duration	Temporal Distribution of Inflow
Baseline	S1	Actual volume	32 days	Uniform distribution
Increased volume	S2	1.5 times	32 days	Uniform distribution
Short duration–high flow	S3	Unchanged	16 days	Uniform distribution
Long duration–low flow	S4	Unchanged	64 days	Uniform distribution
Pulsed replenishment	S5	Unchanged	32 days	70% concentrated during days 9–16
Balanced replenishment	S6	Unchanged	32 days	30% concentrated during days 9–16

3.2.2. Parameter Calibration and Model Validation

Observed water levels in Baiyangdian were used to calibrate the core hydrodynamic parameters [16]. The hydrodynamic model was calibrated using observed water levels from November 2023 and validated using observed water levels from March to April 2024. Figure 2 compares simulated and observed water levels at Shifangyuan Station. For the November 2023 calibration period, the reported MAE, RMSE, NSE, and R^2 were 0.005 m, 0.007 m, 0.924, and 0.92, respectively. Independent validation was limited to water-level observations at Shifangyuan Station during March–April 2024; spatial flow velocities and conservative-tracer transport were not independently validated.

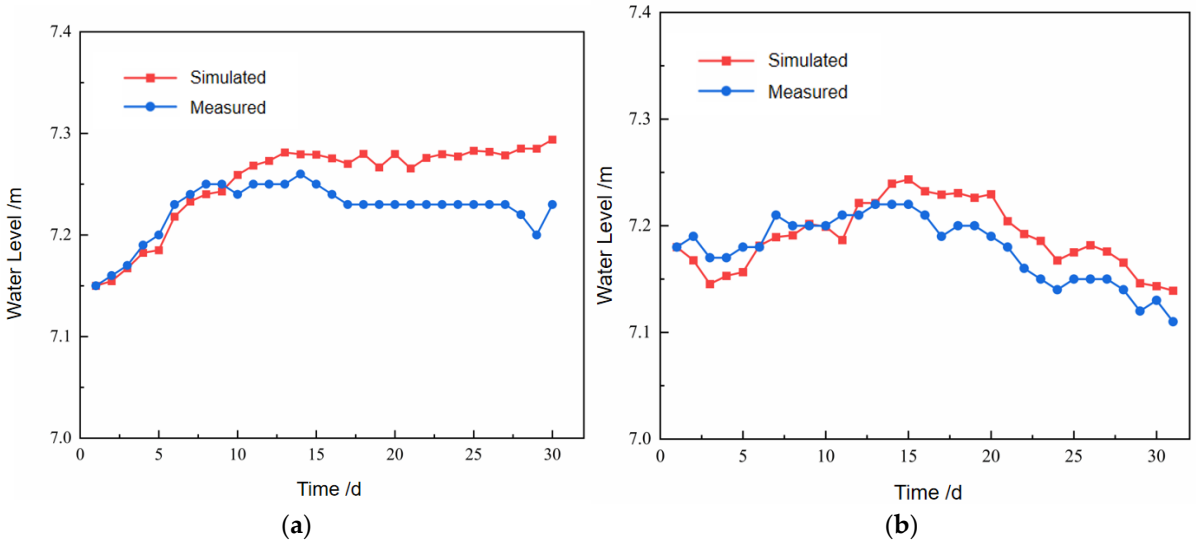


Figure 2. Comparison of simulated and measured water levels in Baiyangdian Lake: (**a**) calibration in November 2023; (**b**) validation in March–April 2024.

The initial and final model settings are summarized in Table 1. The adjusted parameters include the Manning number ($M = 1/n$), the Smagorinsky coefficient, and the constant wind-drag coefficient. Drying, flooding, and wetting depths, together with the maximum CFL number, are listed as fixed numerical settings. The initial water level and sediment seepage rate are also reported separately from the friction and turbulence parameters.

Model parameters were calibrated against observed water levels. The initial and final model settings are summarized in Table 1.

3.3. Simulation Parameter Settings

This study used the actual spring 2024 ecological water replenishment process as the baseline. We then developed six scenarios (Table 2) to examine the effects of changes in total replenishment volume, replenishment duration, and temporal distribution of inflow on the flow field.

S3 and S4 were evaluated at their respective replenishment endpoints, day 16 and day 64, after delivery of the same total water volume. This comparison reflects the joint effects of discharge intensity and replenishment duration. Because discharge intensity and elapsed simulation time vary together, their individual effects cannot be isolated by this endpoint comparison. S5 and S6 used piecewise constant inflows, delivering 70% and 30% of their total volumes, respectively, during days 9–16. The remaining 30% and 70% were distributed uniformly over days 1–8 and 17–32.

The active water zone was operationally defined as the area with simulated flow velocity exceeding 0.006 m s^{-1} (0.60 cm s^{-1}). A common threshold was applied to all scenarios to quantify the spatial extent of relatively active circulation. This study-specific threshold represents an operational classification rather than an independently validated physical or ecological threshold. Threshold sensitivity was not tested. The resulting active water area percentages are therefore conditional on the selected criterion and should not be interpreted as universally applicable indicators of hydrodynamic or ecological performance.

4. Results

4.1. Effects of Total Replenishment Volume on the Flow Field

Figure 3 shows the effects of the increased-volume scenario (S2) and the baseline scenario (S1) on the distribution of the active water zone (flow velocity > 0.60 cm s^{-1}). Under S1, the main-lake area was restricted by microtopography, with a mean flow velocity of only 0.74 cm s^{-1} and the active water zone accounting for 31.37% of the total area. When the total replenishment volume was increased to 1.5 times the baseline value (S2), the mean flow velocity in the main-lake area increased to 0.89 cm s^{-1}, and the active water area fraction increased from 31.37% to 40.71%, an increase of 9.34 percentage points. Spatially, connectivity in Nanliuzhuang was greatly improved, with the active water area fraction increasing by 19.74 percentage points. The water exchange percentage also showed a positive response (Figure 4). Under S2, the water exchange percentage in the main-lake area reached 39.70% by day 24, exceeding the result achieved by S1 over the full 32-day period, and reached 49.34% by the end of the period. This suggests that sufficient water replenishment is a direct driver of reducing stagnant water areas and accelerating water replacement, consistent with the findings of Yu et al. [7] that total water replenishment can improve water quality in lakes in cold and arid regions.

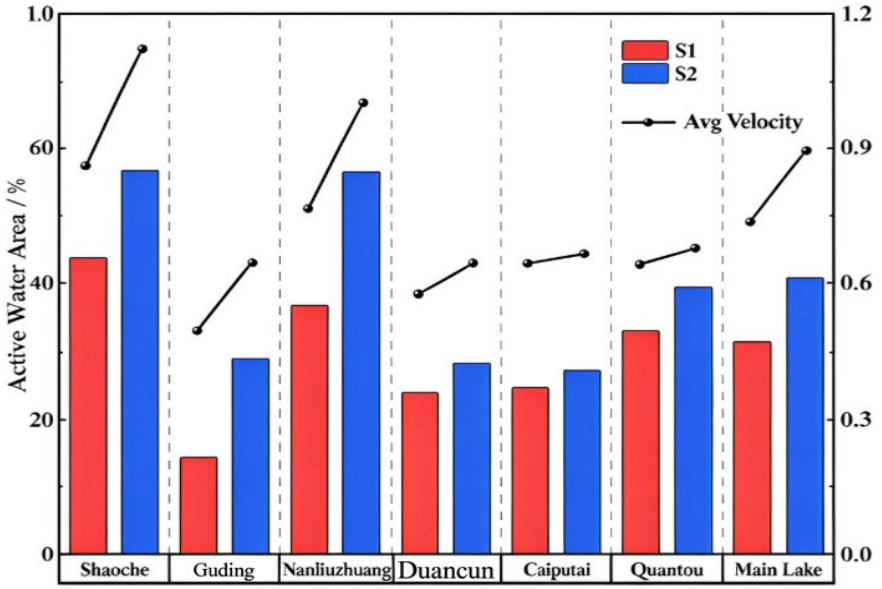


Figure 3. Active water area fractions (bars, left axis) and mean flow velocities (points, right axis) in the main lake and subregions under S1 (red) and S2 (blue). Within each region, the left and right velocity points correspond to the red and blue scenarios, respectively.

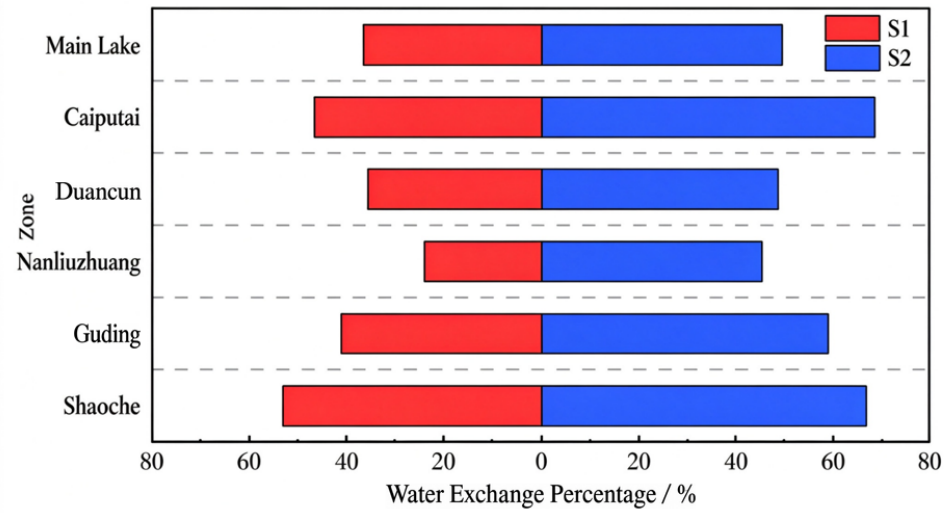


Figure 4. Water exchange percentages in the main lake and subregions under S1 and S2. Percentages represent the proportion of the assessed water area satisfying $C/C_0 \leq 1/e$ (approximately 0.37). Both sides show positive exchange percentages; bar direction distinguishes scenarios.

4.2. Decoupling Between Hydrodynamics and Water Exchange Under Different Replenishment Durations

With the same total replenishment volume, S3 and S4 showed contrasting hydrodynamic and water exchange responses at their respective replenishment endpoints, on days 16 and 64 (Figures 5 and 6). These differences reflect the combined effects of discharge intensity and elapsed simulation time. In terms of hydrodynamics, S3 (short duration–high flow) had much greater driving kinetic energy than S4 (long duration–low flow). The mean flow velocity in the main-lake area was 1.05 cm s^{-1} under S3, which was 75% higher than that under S4 (0.60 cm s^{-1}), while the active water area fraction approached 50%.

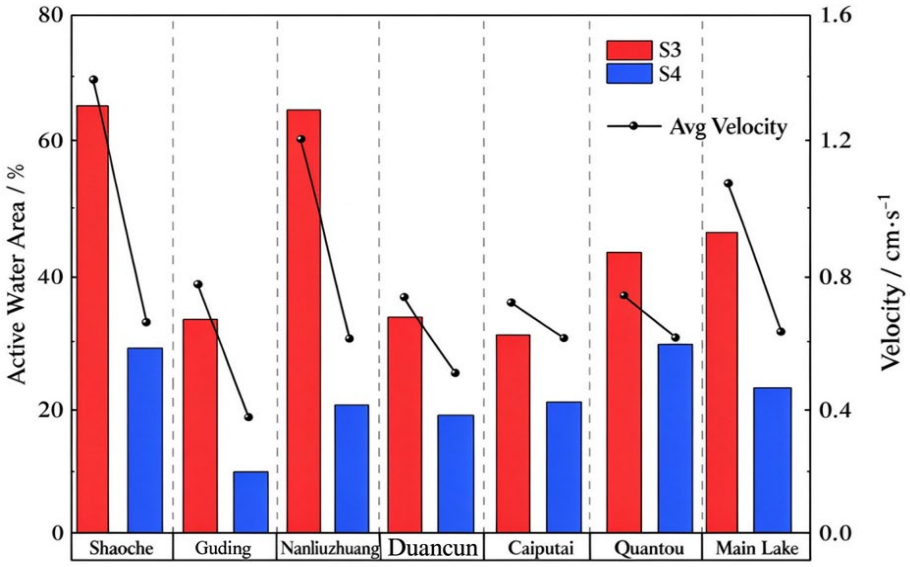


Figure 5. Active water area fractions (bars, left axis) and mean flow velocities (points, right axis) in the main lake and subregions under S3 (red) and S4 (blue). Within each region, the left and right velocity points correspond to the red and blue scenarios, respectively.

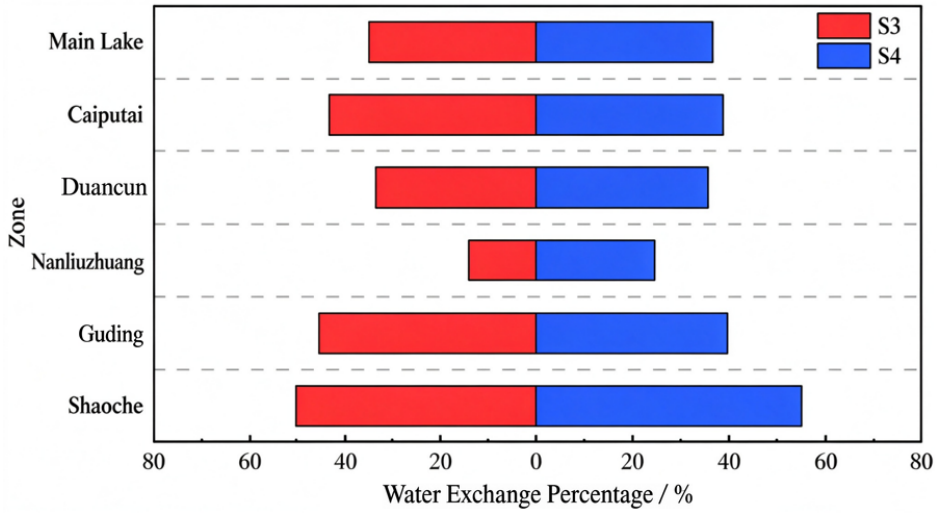


Figure 6. Area-based water exchange percentages ($C/C_0 \leq 1/e$) in the main lake and subregions at the replenishment endpoints of S3 (day 16) and S4 (day 64). Both sides show positive exchange percentages; bar direction distinguishes scenarios.

However, the response of water exchange percentages to changes in replenishment duration showed strong spatial heterogeneity. The simulated main-lake water exchange percentages were 36.61% under S4 on day 64 and 34.83% under S3 on day 16. This 1.78-percentage-point difference should be interpreted cautiously because the evaluation times differ and quantitative uncertainty bounds are unavailable. In Gudingdian and Caiputai, the reported water exchange percentages under S3 were approximately 5 percentage points higher than under S4. The higher endpoint exchange percentages under S4 in some subregions may reflect longer elapsed time and differences in transport pathways [18]. The water exchange percentage in Nanliuzhuang was 10.67 percentage points higher under S4 than under S3. These spatially contrasting responses suggest that the relationship between hydrodynamic intensity and water exchange is modulated by local topographic conditions [11].

4.3. Effects of the Temporal Distribution of Inflow

Figures 7 and 8 show the differences between pulsed replenishment (S5) and balanced replenishment (S6) over the same duration. The active water area fraction was 2.38–11.09 percentage points higher under S5 than under S6 across the assessed regions. In terms of water exchange, although the main-lake water exchange percentages were similar under S5 and S6 (about 37%), their responses at the subregional level were quite different. The pulse in S5 promoted deeper water mixing in the topographically complex Gudingdian and Duancun areas, where water exchange percentages reached 47.35% and 37.16%, respectively. In Caiputai, although the final water exchange percentages under both scenarios were 43.00%, the area in a "transitional mixing state" (conservative tracer concentration of 0.37–0.50 mg L^{-1}) under S5 was 34% larger than that under S6. The 0.37–0.50 mg L^{-1} range refers to absolute tracer concentrations. Given C_0 = 1 mg L^{-1}, its limits correspond to dimensionless C/C_0 values of 0.37 and 0.50. This class indicates partial tracer dilution rather than fulfillment of the water renewal criterion, $C/C_0 \leq 1/e$. This suggests that pulsed water replenishment may be more effective in reaching and diluting deeply stagnant water areas [16].

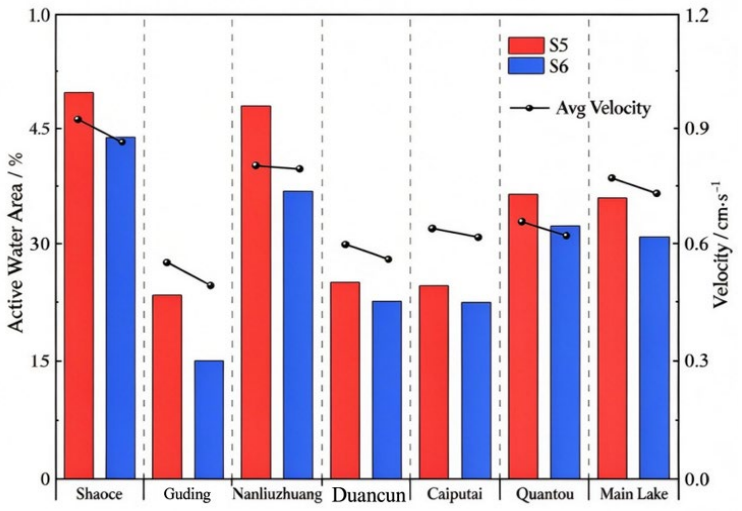


Figure 7. Active water area fractions (bars, left axis) and mean flow velocities (points, right axis) in the main lake and subregions under S5 (red) and S6 (blue). Within each region, the left and right velocity points correspond to the red and blue scenarios, respectively.

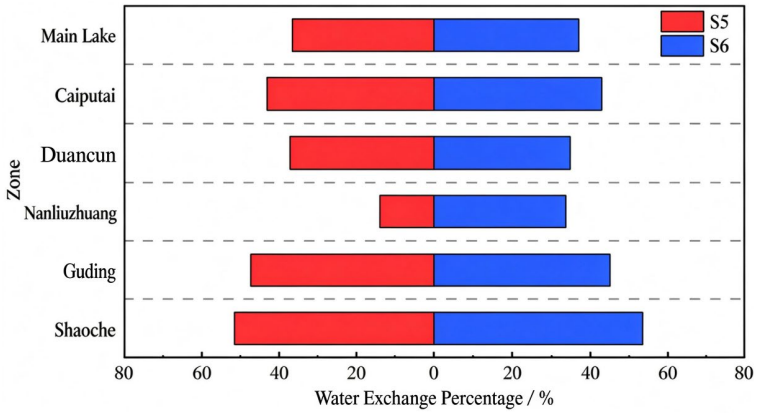


Figure 8. Water exchange percentages in the main lake and subregions under S5 and S6. Percentages represent the proportion of the assessed water area satisfying $C/C_0 \leq 1/e$ (approximately 0.37). Both sides show positive exchange percentages; bar direction distinguishes scenarios.

5. Discussion

5.1. Hydrodynamic Responses to Replenishment Strategies

Due to the historical impact of agricultural reclamation, the Baiyangdian area shows a highly fragmented spatial topological structure. This study found that the increase in simulated flow velocity (S2, S3) can effectively expand the extent of the active water zone (Figure 9). Under pulsed replenishment (S5), changes in active water area and mean velocity differed across subregions. These indicators describe different aspects of hydrodynamic response and should therefore be interpreted together. Transport timescale concepts [18,19] provide a possible framework for interpreting these differences, with local flow pathways and replenishment duration potentially influencing the relationship between circulation and tracer exchange.

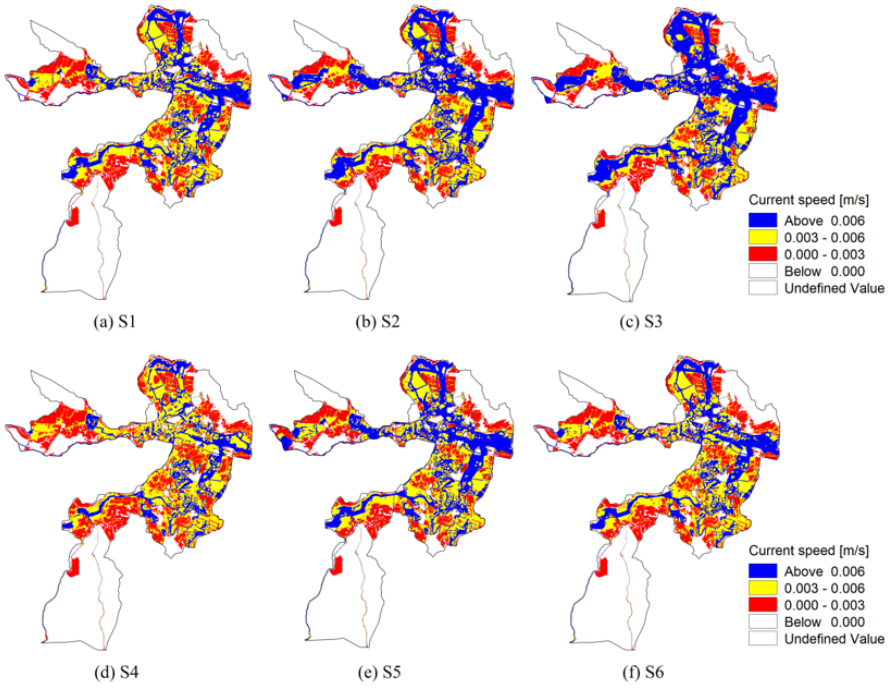


Figure 9. Spatial distributions of simulated mean flow velocity in Baiyangdian Lake under six replenishment scenarios: (**a**) S1, baseline replenishment; (**b**) S2, increased replenishment volume; (**c**) S3, short-duration, high-discharge replenishment; (**d**) S4, long-duration, low-discharge replenishment; (**e**) S5, pulsed replenishment; (**f**) S6, balanced replenishment.

5.2. Water Exchange Analysis

The simulations suggest that stronger hydrodynamic conditions do not consistently produce higher water exchange percentages and that subregional responses vary with local topographic conditions.

In Shaochedian, S4 produced a higher water exchange percentage at its respective replenishment endpoint than S3. This pattern may reflect differences in flow pathways and elapsed time [18] and does not establish an independent benefit of longer replenishment duration.

Local topographic constraints may contribute to the contrasting subregional responses [11]. Changes in water exchange following large-scale land reclamation have also been reported in a bay [27], although differences in geometry and hydrological conditions limit direct comparison with Baiyangdian. During days 9–16, the mean inflow under S5 was approximately 2.33 times that under S6, with equal total replenishment volumes and durations. The active water area fraction increased by 2.38–11.09 percentage points

under S5 relative to S6. These results suggest that concentrated replenishment may enhance local transport and water exchange in some topographically constrained areas. The tracer concentration patterns in Figure 10 are consistent with spatially variable water exchange. This interpretation can be discussed in relation to Junk et al.'s flood-pulse concept [28] and Chen et al.'s study of dam-induced changes in flood pulses [29]. Xiao et al. [30] examined river morphology and self-purification using water-quality observations, providing a complementary ecological perspective.

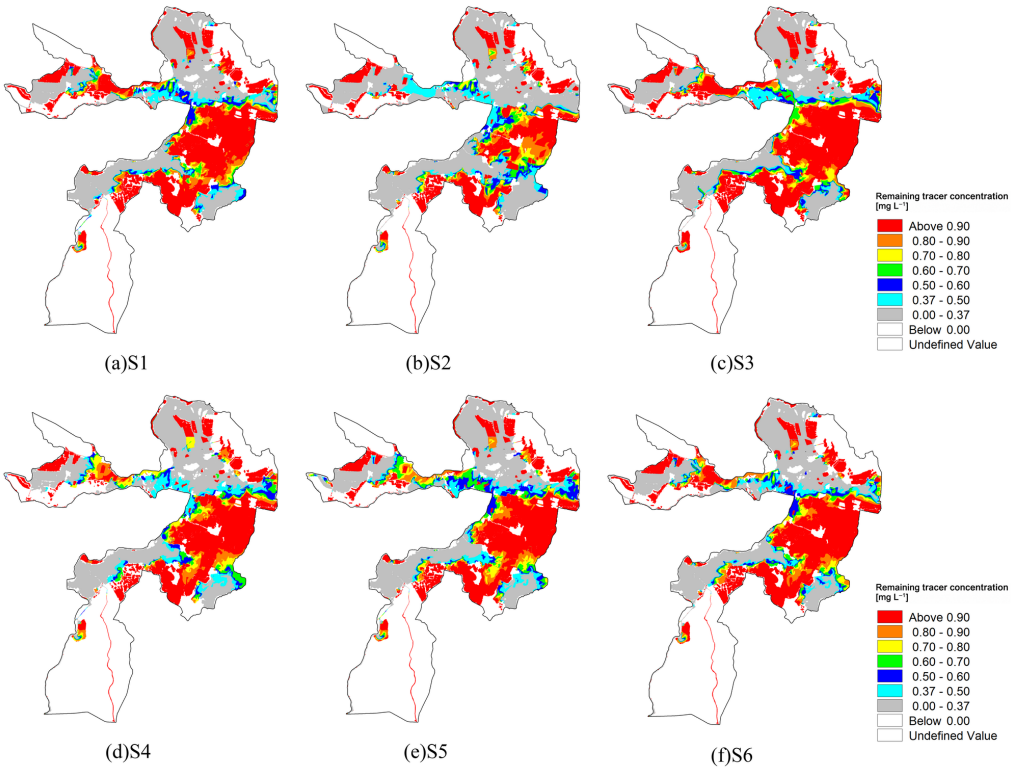


Figure 10. Remaining tracer concentration (mg L^{-1}; C_0 = 1 mg L^{-1}) under S1–S6 (**a**–**f**) at their respective replenishment endpoints: day 32 (**a**,**b**,**e**,**f**), day 16 (**c**), and day 64 (**d**), measured from simulation start. Lower concentrations indicate greater tracer dilution; the 0.37 mg L^{-1} class boundary approximates C_0/e. White represents below-range (<0 mg L^{-1}) or undefined values, which are not distinguished in this display.

5.3. Methodological Limitations and Management Implications

Water exchange predictions may be influenced by uncertainties in bathymetry, bed resistance, boundary discharge, tracer dispersion, and initial conditions. Studies of nonstationary runoff in the Yellow River Basin [31] and depth-dependent soil-moisture responses on the Loess Plateau [32] provide broader hydrological context for future lake–catchment modeling. In a fragmented lake such as Baiyangdian, the representation of channels and embankments may affect simulated flow pathways and hydraulic connectivity. Resistance and dispersion parameters also influence tracer transport and the area meeting the renewal criterion. Consequently, small differences among scenario predictions should be interpreted in the context of model configuration and input uncertainty. The 1.78-percentage-point difference between S3 and S4 does not establish a robust advantage of either strategy, given the absence of quantitative uncertainty estimates and the different evaluation times. Interpretation of scenario differences should also account for the different endpoint times of S3 and S4 and the threshold dependence of active water area. Management implications are therefore conditional on these evaluation choices, as well as the model inputs and parameters.

Shi et al. [16] examined long-term water exchange together with water-quality conditions. Our event-scale analysis focuses on hydrodynamic and conservative-tracer responses. Comparisons should account for differences in evaluation periods and indicator definitions, and ecological implications require site-specific water-quality and biological evidence. Sustainable water replenishment management requires coordinated lake-wide scheduling that accounts for hydraulic connectivity, water availability, conveyance capacity, operating water levels, and available control structures.

6. Conclusions

This study used a two-dimensional hydrodynamic model of Baiyangdian to quantify the simulated responses of lake circulation and water exchange to different ecological water replenishment strategies. The main conclusions are as follows.

Increasing replenishment volume to 1.5 times the baseline raised the main-lake active water area fraction (defined here as flow velocity > 0.60 cm s^{-1}) from 31.37% to 40.71%, with an area-based water exchange percentage of 49.34% on day 32. Shortening the replenishment duration or applying pulsed replenishment expanded the active water zone, although stronger circulation did not consistently correspond to greater water exchange.

Water exchange responses depend on local topographic conditions. The endpoint simulations suggest spatially varying responses to the tested replenishment schedules, providing a basis for further assessment of subregional management options. However, the S3–S4 comparison reflects the combined effects of discharge intensity and elapsed simulation time and does not establish the independent superiority of either strategy. These model-based findings require field verification before practical application.

Author Contributions: Conceptualization, Y.M., L.Z. and Y.Z.; methodology, Y.M., L.Z. and X.L.; validation, Y.M. and Y.G.; formal analysis, Y.M. and L.Z.; investigation, Y.M., Y.Z. and X.L.; resources, Y.M., L.Z. and Y.G.; data curation, Y.M., X.L., Y.C. and Y.Z.; writing—original draft preparation, Y.M. and L.Z.; writing—review and editing, Y.M. and L.Z.; visualization, Y.M. and Y.G.; supervision, Y.G. and Y.C.; project administration, L.Z., Y.Z. and X.L.; funding acquisition, Y.C. All authors have read and agreed to the published version of the manuscript.

Funding: This research was funded by the National Science and Technology Major Project for Comprehensive Environmental Management in the Beijing-Tianjin-Hebei Region (2025ZD1204703), the Natural Science Foundation of Hebei Province (E2025210047, E2025210102), and the Hebei Provincial "Yanzhao Golden Platform" Talent Program (A2025021), Hebei Provincial Central-Guided Local Science and Technology Development Fund Project (246Z5404G,264Z5401G).

Institutional Review Board Statement: Not applicable.

Informed Consent Statement: Not applicable.

Data Availability Statement: The original contributions presented in this study are included in the article.

Acknowledgments: We thank the anonymous reviewers for their constructive comments and helpful suggestions. We also thank Junjie Wang and Chao Xiang of Shijiazhuang Tiedao University for their valuable assistance in revising the manuscript.

Conflicts of Interest: The authors declare no conflicts of interest.

References

1. Han, Q.; Zhou, L.; Sun, W.; Wang, G.; Shrestha, S.; Xue, B.; Li, Z. Assessing alterations of water level due to environmental water allocation at multiple temporal scales and its impact on water quality in Baiyangdian Lake, China. *Environ. Res.* **2022**, *212*, 113366. [CrossRef] [PubMed]

2. Liang, Y.; Gong, Z.; Zhao, Y. Assessing the influence of the ecological restoration project on the submerged aquatic vegetation in the Baiyangdian Lake, northern China. *Ecohydrol. Hydrobiol.* **2024**, *24*, 931–943. [CrossRef]
3. Mao, X.; Liu, L.; Zhao, H. Diatom assemblage shifts in Lake Baiyangdian driven by distinct hydrological changes and yet more eutrophication. *Limnologica* **2024**, *105*, 126155. [CrossRef]
4. Pu, Z.; Bai, J.; Zhang, Q.; Tian, K.; Yang, W.; Zhao, Y.-W. Ecological water replenishment through optimal allocation of lake water in water-scarce areas. *Sci. Total Environ.* **2024**, *956*, 177340. [CrossRef] [PubMed]
5. Zhou, Q.; Chen, H.; Cheng, B.; Cheng, Y.; Guo, B. A study of the effect of lake shape on hydrodynamics and eutrophication. *Sustainability* **2025**, *17*, 1720. [CrossRef]
6. Mao, B.; Wang, X.; Liao, Z.; Miao, Y.; Yan, S. Spatiotemporal variations and tradeoff-synergy relations of ecosystem services under ecological water replenishment in Baiyangdian Lake, North China. *J. Environ. Manag.* **2023**, *343*, 118229. [CrossRef] [PubMed]
7. Yu, H.; Shi, X.; Sun, B.; Zhao, S.; Wang, S.; Yang, Z.; Han, Y.; Kang, R.; Chen, L. Effects of water replenishment on lake water quality and trophic status: An 11-year study in cold and arid regions. *Ecotoxicol. Environ. Saf.* **2024**, *281*, 116621. [CrossRef] [PubMed]
8. Wang, Y.; Liu, G.; Zhu, S.; Hu, W.; Zhang, H.; Zhou, X.; Peng, Z. Assessment of impacts of water transfer on lake flow and water quality in Lake Chaohu using a three-dimensional hydrodynamic-ecological model. *J. Hydrol. Reg. Stud.* **2023**, *46*, 101333. [CrossRef]
9. Zhang, L.; Bai, J.; Zhai, Y.; Zhang, K.; Wang, Y.; Tang, R.; Xiao, R.; Jorquera, M.A. Pollution levels and potential ecological risks of trace elements in relation to bacterial community in surface water of shallow lakes in northern China. *J. Contam. Hydrol.* **2024**, *262*, 104318. [CrossRef] [PubMed]
10. Mao, X.; Zhao, H.; Kattel, G.; Jiang, G.; Ji, Y.; Liu, T.; Yang, J.; Liu, Z.; Wang, C.; Zhao, H.; et al. Both nutrients and macrophytes regulate organic carbon burial: Insights from high-resolution spatiotemporal records of a large shallow lake (Baiyangdian) in eastern China. *Sci. Total Environ.* **2024**, *950*, 175239. [CrossRef] [PubMed]
11. Liu, D.; Wang, X.; Wang, Z.; Zhu, J.; Li, C. Integrated nonstationary and uncertain analysis of coupled relationship of hydrological connectivity and water level in a highly fragmented wetland. *J. Environ. Manag.* **2024**, *360*, 121137. [CrossRef] [PubMed]
12. Zhao, C.; Qian, S.; Meng, C.; Chang, Y.; Guo, W.; Wang, S.; Sun, Y. Blue-green space changes of Baiyangdian Wetland in Xiong'an New Area, China. *Adv. Meteorol.* **2022**, *2022*, 3351916. [CrossRef]
13. Zhang, Y.; Wang, X.; Li, C.; Cai, Y.; Yang, Z.; Yi, Y. NDVI dynamics under changing meteorological factors in a shallow lake in future metropolitan, semiarid area in North China. *Sci. Rep.* **2018**, *8*, 15971. [CrossRef] [PubMed]
14. Li, B.; Yang, G.; Wan, R.; Li, H. Hydrodynamic and water quality modeling of a large floodplain lake (Poyang Lake) in China. *Environ. Sci. Pollut. Res.* **2018**, *25*, 35084–35098. [CrossRef] [PubMed]
15. Dai, J.; Wu, S.; Wu, X.; Lv, X.; Sivakumar, B.; Wang, F.; Zhang, Y.; Yang, Q.; Gao, A.; Zhao, Y.; et al. Impacts of a large river-to-lake water diversion project on lacustrine phytoplankton communities. *J. Hydrol.* **2020**, *587*, 124938. [CrossRef]
16. Shi, X.; Wang, S.; Zhao, S.; Sun, B.; Yu, H.; Zhang, F.; Zhang, Q. Evaluating the effects of ecological water replenishment on lake water exchange in semi-arid regions insights from an 11-year modeling study. *J. Environ. Manag.* **2025**, *391*, 126491. [CrossRef] [PubMed]
17. Fourniotis, N.T.; Leftheriotis, G.A. Water renewal simulation in two flow-through water bodies in western Greece. *Water* **2023**, *15*, 2745. [CrossRef]
18. Monsen, N.E.; Cloern, J.E.; Lucas, L.V.; Monismith, S.G. A comment on the use of flushing time, residence time, and age as transport time scales. *Limnol. Oceanogr.* **2002**, *47*, 1545–1553. [CrossRef]
19. Shen, X.; Detenbeck, N.; You, M. Spatial and temporal variations of estuarine stratification and flushing time across the continental U.S. *Estuar. Coast. Shelf Sci.* **2022**, *279*, 108147. [CrossRef] [PubMed]
20. Zhu, J.; Gong, Z.; Wang, Y. Rapid response of aquatic ecosystems and environment in shallow macrophytic lakes to large-scale cofferdam removal. *Ecol. Indic.* **2025**, *178*, 113884. [CrossRef]
21. Fu, X.; Yang, W.; Zheng, L.; Liu, D.; Li, X. Spatial patterns of macrobenthos taxonomic and functional diversity throughout the ecotones from river to lake. *Front. Ecol. Evol.* **2022**, *10*, 922539. [CrossRef]
22. Liu, Y.; Zhang, Q. Study on the spatiotemporal variation in and driving mechanism of water quality in Baiyangdian Lake. *Water* **2024**, *16*, 166. [CrossRef]
23. Xu, P.; Zhang, L.; Zhang, X.; Mao, Z.; Rao, L.; Yang, J.; Zhou, Y. Simulation of water renewal time in West Lake based on Delft3D and its environmental impact analysis. *Water* **2025**, *17*, 2847. [CrossRef]
24. Xu, P.; Zhang, X.; Zhang, L.; Wang, Q.; Mao, Z.; Rao, L.; Yang, J.; Zhou, Y. Impact of artificial water replenishment on spatiotemporal distribution of local water renewal time in West Lake. *Water* **2025**, *17*, 3563. [CrossRef]
25. Yu, J.Z.; Liu, D.; Wang, X.; Zhu, J.; Liao, Z.M.; Cai, C.Y. A transition zone boundary determining method based on MIKE21: A case study of Baiyangdian Lake, North China. *J. Hydrol.* **2024**, *638*, 131447. [CrossRef]
26. Oubarka, I.; Kissami, I.; Elmahi, I.; Deleersnijder, E. A robust and well-balanced finite volume solver for investigating the effects of tides on water renewal timescale in the Nador lagoon, Morocco. *Math. Comput. Simul.* **2024**, *226*, 511–523. [CrossRef]

27. Liu, L.; Li, Y.; Yuan, D.; Li, X.; Mao, Y.; Zhao, F. Variations in water exchange in the sub-areas of a bay following large-scale land reclamation. *Mar. Pollut. Bull.* **2024**, *208*, 116998. [CrossRef] [PubMed]
28. Junk, W.J.; Bayley, P.B.; Sparks, R.E. The flood pulse concept in river-floodplain systems. *Can. Spec. Publ. Fish. Aquat. Sci.* **1989**, *106*, 110–127.
29. Chen, L.; Wu, Y.; Xu, Y.; Zhang, G. Alteration of flood pulses by damming the Nenjiang River, China—Implication for the need to identify a hydrograph-based inundation threshold for protecting floodplain wetlands. *Ecol. Indic.* **2021**, *124*, 107406. [CrossRef]
30. Xiao, C.; Chai, Z.; Chen, D.; Luo, Z.; Li, Y.; Ou, Q.; Zhang, Y. Research on the influence of river morphological changes on water self-purification capacity: A case study of the Shiwuli River in Chaohu Basin. *Water* **2025**, *17*, 1694. [CrossRef]
31. Wang, J.; Chi, Y.; Zhang, S.; Shi, B.; Zhang, L.; Du, C.; Li, X.; Li, B.; Yang, L.; Huang, L.; et al. Quantitative attribution of seasonal runoff variations in the Yellow River Basin under unsteady conditions using a modified Budyko framework. *J. Hydrol.* **2026**, *675*, 135588. [CrossRef]
32. Wang, J.; Zhang, S.; Chi, Y.; Shi, B.; Li, X.; Li, B.; He, P. Divergent hydrological responses of multi-depth soil moisture variability to multiple factors on the Loess Plateau, China. *J. Hydrol.* **2026**, *670*, 135226. [CrossRef]

Disclaimer/Publisher's Note: The statements, opinions and data contained in all publications are solely those of the individual author(s) and contributor(s) and not of MDPI and/or the editor(s). MDPI and/or the editor(s) disclaim responsibility for any injury to people or property resulting from any ideas, methods, instructions or products referred to in the content.